Simulation of the octopod robot controlled by different Central Patterns Generators

Dariusz Grzelczyk, Bartosz Stańczyk, Olga Szymanowska, Jan Awrejcewicz

Abstract: In this paper we focus on kinematic simulation of the octopod robot during its walking on a flat and hard surface. The robot legs are kinematically excited by different well-known mechanical non-linear oscillators as well as new (proposed) ones, working as Central Pattern Generators (CPGs). Time histories of kinematic parameters of the octopod locomotion process are obtained. In particular, we considered displacement and velocity fluctuations of the robot gravity centre in different directions. Eventually, some advantages of the proposed CPGs are outlined, i.e. the lack of the acceleration and deceleration of the robot gravity centre, minimisation of the ground reaction forces between the robot and the ground as well as low energy consumption of the robot during walking.

1. Introduction

Investigations of walking machines were initiated in 1960s by McGhee and Frank who constructed the first four-legged robot called "Phoney Pony" [1]. Since that time, a wide spectrum of quadruped (four-legged) robots have been built. At the same time, six-legged robots have been also constructed and investigated. For instance, interesting state-of-the-art in this area can be found in references [2, 3], where a summary related to biological paragon from nature, methods of studies of animals locomotion and the constructed walking robots are discussed. Recently, also eight-legged robots have become very popular, for instance: a biomimetic eight-legged robot SCORPION [4], eight-foot robot named OctoRoACH [5], and searching and rescuing robot Halluc II [6].

In one of our recent papers [3], we introduced the prototype of the hexapod robot designed based on the biomechanics of insects for inspection and operation applications. In that paper a detailed discussion on the mechanical construction, electronic control system, devices installed on the robot body and the control problem of the robot legs are presented. Finally, we proposed other model of CPG based on the oscillator describing stick-slip induced vibrations. Both numerical and experimental results showed some analogies between the characteristics of the simulated walking robot and animals met in nature. Furthermore, the benefits of the proposed stick-slip vibrations as a CPG are outlined. In our other paper [7] we focused on the kinematic, dynamic and power consumption analysis of the second version of the hexapod robot. The same stick-slip oscillator working as a CPG was investigated from the viewpoint of fluctuations of the robot gravity centre both in vertical and movement direction, ground reaction forces between the robot legs and the ground as well as energy demand of the whole robot during walking. Time histories of the key kinematic and dynamic quantities describing locomotion of the robot were studied numerically and verified experimentally. Also, we showed the benefits of the proposed stick-slip oscillator working as a CPG. On the contrary to the previous references [3, 7], in the present paper we investigate kinematics of the walking octopod robot controlled by different CPGs. For this purpose, we use previously developed methods and models for robot leg control and models describing kinematic parameters of the robot. However, we propose another CPG model based on sine function which makes it possible to control the movement of the robot legs in simple way, and is easy to generate by both computer software and electronic circuits. In addition, numerical results were also obtained for other CPGs (Toda-Rayleigh lattice and the proposed CPG model) and other values of parameters describing the analyzed robot and parameters of the single robot stride. Finally, we showed that the proposed CPG model based on the sine function can be most efficient with respect to kinematic (and dynamic) parameters of the robot and its energy demand during walking.

2. The prototype of the octopod robot

The CAD project of the considered octopod robot is presented in Fig. 1. To develop the presented model, we used CAD three-joint leg mechanism of the hexapod robot leg and definitions of its links and joints, which can be found in references [3, 7]. The developed virtual model can be useful for design optimization and virtual experiments of the robot motion. The mechanical design of the robot focuses on two main components, i.e. the body and the legs. The full size of the CAD model of the robot is about 590 mm × 370 mm × 150 mm (length × width × height).

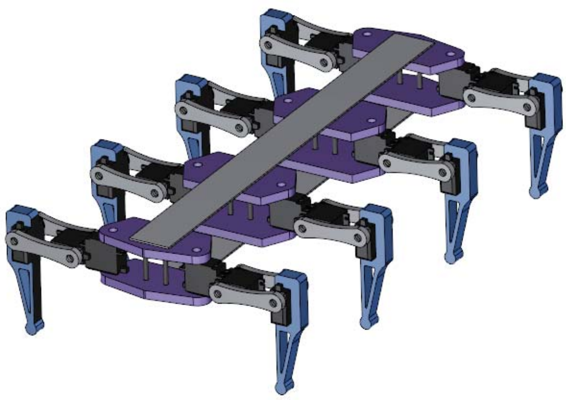

Figure 1. CAD model of the investigated octopod robot created in Inventor.

3. Kinematics of the octopod robot

A kinematic model of the analyzed robot supported by different legs is presented in Fig. 2. In order to obtain this model, we used a method similar to the one presented in our previous papers [3, 7]. The octopod robot is embedded in the Cartesian coordinate system xyz, in the gravity field of the Earth, and it is supported by four legs which form the support polygon (quadrangle) of the robot. Eight identical legs of the robot are denoted as L1, L2, L3, L4 (on the left side of the robot) and R1, R2, R3, R4 (on the right side of the robot). Distances between the ground and the robot gravity centre are denoted by $h_a(t)$, $h_b(t)$. Due to symmetry of the considered robot, it can be assumed that the contact forces $R(t)$ are the same in each robot legs (see Fig. 2). Moreover, we assumed relatively large friction between the robot legs and the ground, which is required to prevent the legs from sliding during walking.

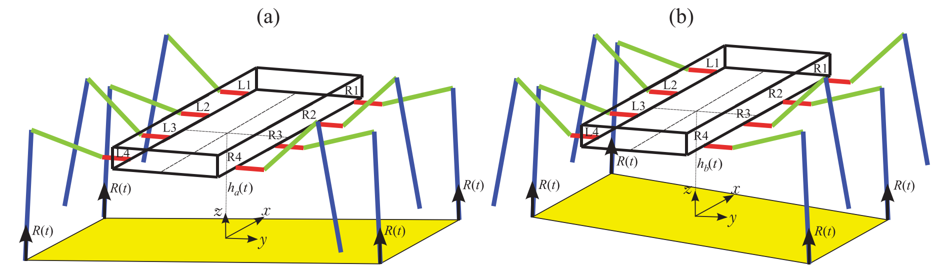

Figure 2. Model of the octopod robot in two different gait configuration: (a) the robot supported by the legs R1, R3, L2 and L4; (b) the robot supported by the legs L1, L3, R2 and R4.

As can be seen, in this model the robot legs are divided into two groups, i.e. the group *a* (legs R1, R3, L2 and L4) and group *b* (legs L1, L3, R2 and R4). The movements of all robot legs are controlled by the same CPG, however, the signals applied to the group *b* of the legs are in anti-phase with respect to signals applied to the group *a*. As a result, the robot is supported by the legs from the group *a* (Fig. 2a) in one phase and by the legs from the group *b* (Fig. 2b) in the other one. Each of the robot legs contains three links of the lengths $l_1 = 40\,\text{mm}$, $l_2 = 70\,\text{mm}$ and $l_3 = 120\,\text{mm}$, which correspond to the Coxa, Femur and Tibia, respectively.

4. Control of the robot leg movements by CPGs

The first CPG model was proposed in 1980s by Cohen et al. through the study on the dissection of a lamprey spinal cord [8]. Since then, numerous investigators have been applying the CPG algorithms to control different bio-inspired walking multi-legged robots. A brief literature review devoted to the implementation of CPG algorithms to control hexapod motion can be found, for instance, in references [3, 9, 10].

Below we consider the first three popular non-linear mechanical oscillators described by non-dimensional ordinary differential equations (ODEs) and working as a CPGs, namely: Hopf oscillator, van der Pol oscillator and Toda-Rayleigh lattice. A simple Hopf oscillator is governed by the first-order ODEs

$$\begin{cases} \dot{X} = (\mu - X^2 - Z^2)X + \omega Z, \\ \dot{Z} = (\mu - X^2 - Z^2)Z - \omega X, \end{cases} \tag{1}$$

van der Pol oscillator is described by the first-order ODEs

$$\begin{cases} \dot{X} = Z, \\ \dot{Z} = \mu(1 - X^2)Z - \omega^2 X, \end{cases} \tag{2}$$

whereas the Toda-Rayleigh lattice is governed by the first-order ODEs

$$\begin{cases} \dot{X}_1 = Z_1, \\ \dot{Z}_1 = \omega^2 (e^{X_2 - X_1} - e^{X_1 - X_2}) + \mu(1 - Z_1^2) Z_1, \\ \dot{X}_2 = Z_2, \\ \dot{Z}_2 = \omega^2 (e^{X_1 - X_2} - e^{X_2 - X_1}) + \mu(1 - Z_2^2) Z_2. \end{cases} \tag{3}$$

Stable orbits of these oscillators obtained for fixed values $\omega = 2$, $\mu = 6$ and different initial conditions (marked with squares) are presented in Fig. 3. The obtained trajectories oscillate stably, and therefore they were often used to generate the trajectory of a leg tip of robot legs. By changing the values of parameters μ and ω, we can change the shape of the stable orbit and its period. As a result, we can control the parameters of the single robot stride. However, the obtained trajectories cannot be directly used to control the robot leg. They must be converted to the workspace of the leg mechanism first, and then to the joints space of the leg using inverse kinematics relationships.

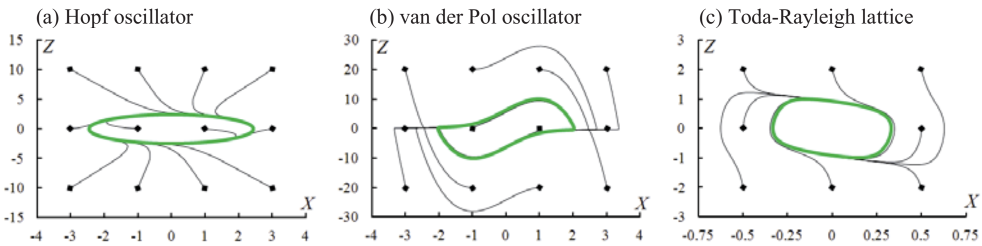

Figure 3. Phase trajectories of three different typical non-linear oscillators for $\omega = 2$, $\mu = 6$ and various initial conditions.

Motivated by investigations of a trajectory of a leg tip of real insects and different biologically inspired robots, we propose other generator based on the sine function, further referred to as a SINE generator. The proposed model is described by the relations

$$X_2(t) = \begin{cases} \frac{2}{\pi}\text{modulo}(\omega t, \pi) & \text{if} \quad 0 < \text{modulo}(\omega t, 2\pi) \le \frac{\pi}{2}, \\ 1 - \frac{2}{\pi}\text{modulo}\left(\omega t - \frac{\pi}{2}, \pi\right) & \text{if} \quad \frac{\pi}{2} < \text{modulo}(\omega t, 2\pi) \le \frac{3}{2}\pi, \\ -1 + \frac{2}{\pi}\text{modulo}\left(\omega t - \frac{3}{2}\pi, \pi\right) & \text{if} \quad \frac{3}{2}\pi < \text{modulo}(\omega t, 2\pi) \le 2\pi, \end{cases} \tag{4}$$

$$Z_2(t) = \left|\sin^2\left(\omega t + \frac{\pi}{2}\right)\right| \cdot \mathbf{1}\left(-\sin\left(\omega t + \frac{\pi}{2}\right)\right), \tag{5}$$

$$X_1(t) = -X_2(t), \tag{6}$$

$$Z_1(t) = -Z_2(t), \tag{7}$$

where $\mathbf{1}\left(-\sin\left(\omega t + \frac{\pi}{2}\right)\right)$ is the classical step function. The stable orbit for the proposed SINE generator is presented in Fig. 4, and it resembles the shape of the trajectory of a leg tip of a real stick insect presented in references [11, 12].

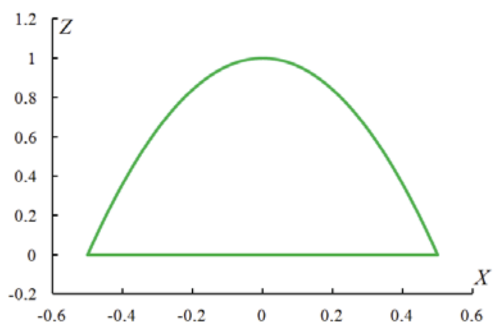

Figure 4. Phase trajectories of the proposed SINE generator.

The presented phase trajectories of the considered oscillators can be applied to control the leg tip of the robot. The size and shape of these trajectories have a great impact on the length and height of a single robot stride, while the orbit period corresponds to the period of the single robot stride. As a result, it is possible to change the gait parameters by changing parameters of the used CPG model, or converting the trajectory of CPG into the workspace of the robot leg [3, 7]. The patterns of the stable orbits of four considered CPG models are depicted in Fig. 5a. By multiplying the variables X and Z of an oscillator working as a CPG, we are able to change directly both the length and height of the single robot stride. The examples of the trajectories of CPG scaled to the workspace of the robot leg mechanism are presented in Fig. 5b.

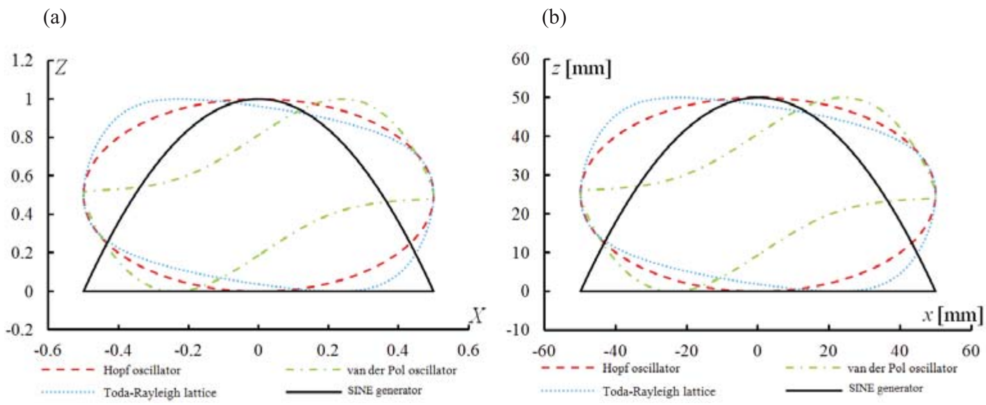

Figure 5. The stable orbits of the investigated CPGs: (a) normalized periodic orbits; (b) the same orbits converted into workspace of the leg mechanism (the stride length $l = 100\,\mathrm{mm}$, the stride height $h = 50\,\mathrm{mm}$).

In further numerical simulations we used variable X of CPG to control the leg tip in x-direction, variable $\dot{X} = Z$ to control the leg tip in the z-direction, whereas the coordinate y of the leg tip is fixed (in this case we used $y = 110\,\mathrm{mm}$).

5. Numerical simulations

In numerical simulations, we applied the standard fourth-order Runge–Kutta method implemented in Scilab. Initial parameters of the considered robot gait are: the stride length $l = 100\,\mathrm{mm}$, the stride height $h = 50\,\mathrm{mm}$ and the stride period $T = 3\,\mathrm{s}$. As a result, the average speed of the robot movement in the forward direction is equal to 0.0667 m/s.

Fig. 6 presents the trajectories plotted by the robot gravity centre $z_C(t)$ in the vertical direction and trajectories plotted by the robot leg tips (group *a* – solid curves, and group *b* – dashed curves). When the three first oscillators controlling the robot legs are applied (see Figs. 6a-c), on the contrary to the results presented in Fig. 6d, considerable fluctuations of the robot gravity centre are clearly observed. For Hopf oscillator, van der Pol oscillator and Toda-Rayleigh lattice, the gravity centre is periodically moved up and down and varies in the range of about a half of the stride height, whereas no fluctuations are observed if the proposed SINE generator is used. As can be seen, the proposed CPG model does not have the mentioned disadvantages, because the robot gravity centre is at a constant level in each phase of its motion.

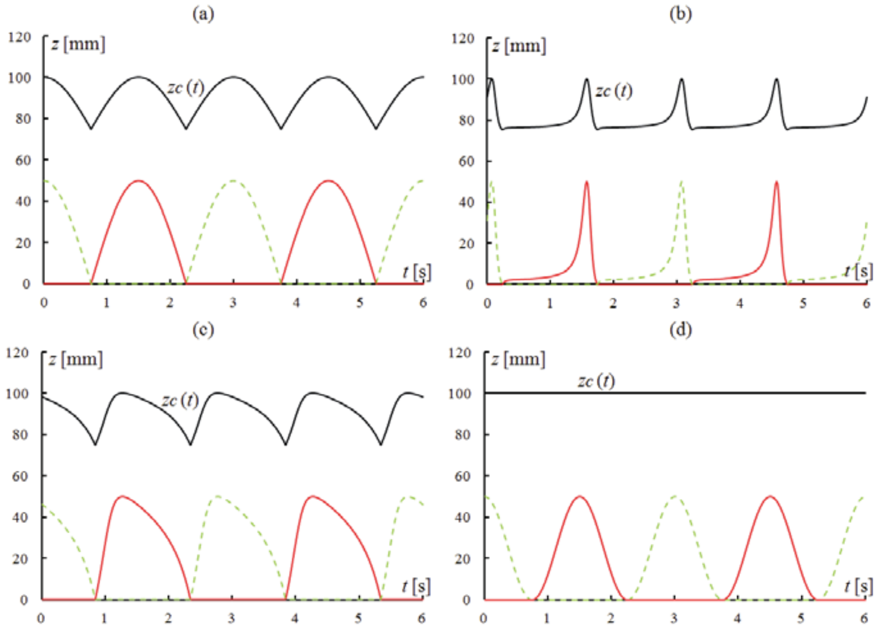

Figure 6. Fluctuation curves of the robot gravity centre $z_C(t)$ and trajectories plotted by the robot legs for different CPGs (solid curves denote group *a* of the robot legs, whereas dashed curves denote group *b* of the robot legs): (a) Hopf oscillator; (b) van der Pol oscillator; (c) Toda-Rayleigh lattice; (d) SINE generator.

Displacement curves of the robot gravity centre in both z and x direction, obtained for different CPGs, are presented in Fig 7. The adequate results regarding the velocity curves (obtained by numerical differentiation of the displacement curves) are presented in Fig. 8. Analysis of the results presented in Figs. 6-8 indicates that in the cases of Hopf oscillator, van der Pol oscillator and Toda-Rayleigh lattice, there exist such phases of the robot motion in which the distance between the centre of the coordinate system and the leg tips touching the ground changes significantly. Moreover, for the van der Pol oscillator some periods of the robot motion are realized faster, while others slower, and therefore the presented fluctuations of the robot gravity centre are the largest for this CPG model. In this case, we can observe the greatest unnecessary accelerations and decelerations of the robot gravity centre in both forward and vertical directions. In the case of the proposed SINE generator working as a CPG, fluctuations of the gravity centre of the robot in any phase of its movement are not observed. It should be noted that the velocities of the robot gravity centre have been obtained by simple numerical differentiation of the displacement variations, and therefore can be slightly different from reality. However, the presented results show characteristic fluctuation of the robot velocity (twice per one robot stride), which are not detected for the proposed CPG model.

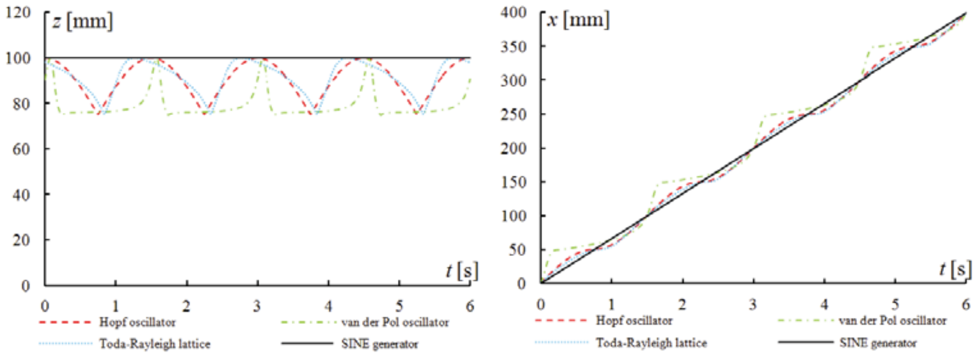

Figure 7. Fluctuations of the displacement curves of the robot gravity centre obtained numerically for different CPGs: (a) in z direction; (b) in x direction.

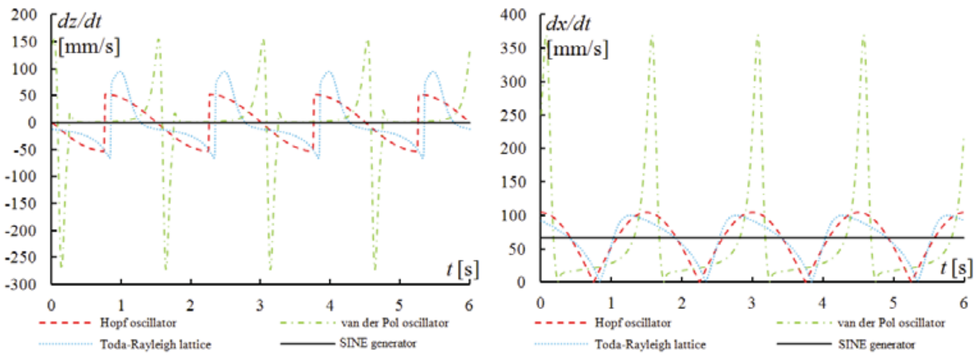

Figure 8. Fluctuations of the velocity curves of the robot gravity centre obtained numerically for different CPGs: (a) in z direction; (b) in x direction.

It should be noted that the fluctuations of the robot gravity centre presented in Figs. 6-8, due to its acceleration/deceleration in the vertical direction, have a great impact on the contact forces acting on the robot legs. Due to the mentioned fluctuation of the robot, the values of reaction forces oscillate (increase and decrease) around the reaction force resulting from the weight of the robot. Therefore, the most frequent and the largest oscillations of contact forces occur in the case of the van der Pol oscillator, while the lowest fluctuations of contact forces exist when the proposed SINE generator is applied.

It should be also noted that power consumption belongs to one of the main operational restrictions on autonomous walking machines. During the last three to four decades, numerous researchers have been also exploring power consumption optimization techniques for these walking robots [13-15]. Fluctuations of the gravity centre and unnecessary changes of speed and acceleration in the moving direction of the robot can have a great impact on energy costs during walking process of the robot.

For this reason, the variation curves of the gravity centre and acceleration of the robot in moving direction should be relatively small during typical walking process of the robot. Therefore, the proposed SINE generator working as a CPG allows for relatively low energy consumption during walking of the robot.

6. Conclusions

A biologically-inspired CAD model of the octopod robot is presented and modelled to study kinematic parameters describing the robot locomotion. The walking process of the considered robot on a flat and hard ground is realized by four different CPG models. A choice of a relatively hard ground has its justification, since this kind of surface generates greater contact forces when the robot legs touch the ground.

The proposed SINE generator based on the sine function is relatively simple in comparison with other control methods presented in the literature and it is useful especially in cases when robot walks on the flat, regular surfaces. We showed that the choice of the applied CPG has a great impact on the kinematical (and dynamical) parameters of the robot gait. The model of CPG constructed based on the van der Pol oscillator appears to be the worst, because the largest unnecessary accelerations and decelerations, both in the vertical and horizontal (movement) directions of the robot, have been detected. As a result, the mentioned fluctuations have a great impact on the energy consumption during walking. That is why during normal walking both the variation curves of the gravity centre and acceleration of the robot in the movement direction should be possibly close to zero. The robot controlled by the proposed CPG does not have unnecessary fluctuations of the gravity centre and low acceleration/deceleration in moving direction. As a result, this generator can be more efficient from the viewpoint of energy cost in comparison to other CPGs. The obtained information can be useful for further analysis of the strength and structural stability of the whole robot and its legs, trouble-free use as well as extension of life and operating time of the robot.

Acknowledgments

The work has been partially supported by the National Science Centre of Poland under the grant OPUS 9 no. 2015/17/B/ST8/01700 for years 2016-2018.

References

[1] McGhee, R., Frank, A. On the stability properties of quadruped creeping gaits. *Mathematical Biosciences* 3, (1968), 331-351.

[2] Chen, X., Wang, L., Ye, X., Wang, G., Wang, H. Prototype development and gait planning of biologically inspired multi-legged crablike robot. *Mechatronics* 23, (2013), 429-444.

[3] Grzelczyk, D., Stańczyk, B., Awrejcewicz, J. Prototype, control system architecture and controlling of the hexapod legs with nonlinear stick-slip vibrations. *Mechatronics* 37, (2016), 63-78.

[4] Klaassen, B., Linnemann, R., Spenneberg, D., Kirchner, F. Biomimetic walking robot SCORPION: control and modeling. *Robotics and Autonomous Systems* 41, (2002), 69-76.

[5] Pulliny, A.O., Kohuty, N.J., Zarrouk, D., Fearing, R.S. Dynamic turning of 13 cm robot comparing tail and differential drive. *Proceeding of 2012 IEEE International Conference on Robotics and Automation*, Minnesota, USA, May 14-18, 2012, 5086-5093.

[6] http://www.pinktentacle.com/2007/07/halluc-ii-8-legged-robot-vehicle/

[7] Grzelczyk, D., Stańczyk, B., Awrejcewicz, J. Kinematics, dynamics and power consumption analysis of the hexapod robot during walking with tripod gait. *International Journal of Structural Stability and Dynamics* 17, (2017), 17 pages.

[8] Cohen, A., Holmes, P., Rand, R. The nature of the coupling between segmental oscillators of the lamprey spinal generator or locomotion: a mathematic model. *Journal of Mathematical Biology* 13, (1982), 345-369.

[9] Chen, W., Ren, G., Zhang, J., Wang, J. Smooth transition between different gaits of a hexapod robot via a central pattern generators algorithm. *Journal of Intelligent & Robotic Systems* 67, (2012), 255-270.

[10] Ijspeert, A. Central pattern generators for locomotion control in animals and robots: a review. *Neural Network* 21, (2008), 642-653.

[11] Durr, V., Schmitz, J., Cruse, H. Behaviour-based modelling of hexapod locomotion: linking biology and technical application. *Arthropod Structure & Development* 33, (2004), 237-250.

[12] Schilling, M., Hoinville, T., Schmitz, J., Cruse, H. Walknet, a bio-inspired controller for hexapod walking. *Biological Cybernetics* 107, (2013), 397-419.

[13] Jin, B., Chen, C., Li, W. Power consumption optimization for a hexapod walking robot. *Journal of Intelligent & Robotic Systems* 71, (2013), 195-209.

[14] Nishii, J. Legged insects select the optimal locomotor pattern based on the energetic cost. *Biological Cybernetics* 83, (2000), 435-442.

[15] Nishii, J. An analytical estimation of the energy cost for legged locomotion. *Journal of Theoretical Biology* 238, (2006), 636-645.

Dariusz Grzelczyk, Ph.D.: Lodz University of Technology, Department of Automation, Biomechanics and Mechatronics, 1/15 Stefanowski Str., 90-924 Lodz, Poland (*dariusz.grzelczyk@p.lodz.pl*).

Bartosz Stańczyk, Ph.D.: Lodz University of Technology, Department of Automation, Biomechanics and Mechatronics, 1/15 Stefanowski Str., 90-924 Lodz, Poland (*bartosz.stanczyk@p.lodz.pl*). The author gave a presentation of this paper during one of the conference sessions.

Olga Szymanowska, Ph.D. Student: Lodz University of Technology, Department of Automation, Biomechanics and Mechatronics, 1/15 Stefanowski Str., 90-924 Lodz, Poland (*olga.szymanowska@dokt.p.lodz.pl*).

Jan Awrejcewicz, Professor: Lodz University of Technology, Department of Automation, Biomechanics and Mechatronics, 1/15 Stefanowski Str., 90-924 Lodz, Poland (*jan.awrejcewicz@p.lodz.pl*).